Estimating Low Frequency Oscillation using Bacterial Swarm Algorithm with Local Probability Likelihood Approach

Wanyu Ye*, Yuefeng Guo*, Tianyao Ji† and Mengshi Li†
*Qingyuan Power Supply Bureau, China Southern Grid, Guangdong, Qingyuan, 511500, China
†School of Electric Power Engineering, South China University of Technology, Guangzhou, 510641, China
Correspondence author: Mengshi Li Email: mengshili@scut.edu.cn

***Abstract*—This paper proposes a Low Frequency Oscillation (LFO) parameters estimation scheme based on Bacterial Swarm Algorithm (BSA). LFO is caused by a wide variety of events, including system faults and load switching. Thus, it is an important task to accurately estimate the parameters of LFO, and further perform fault diagnosis. Although the techniques such as Prony's method could reconstruct the form of the signal, the estimated parameters are not accurate enough. In order to improve the estimation accuracy, this research improves the regression objective function, which aims to minimize the probability likelihood between a segment of the signal filtered by a Mathematica Morphology (MM) filter and its regression. In the experimental studies, BSA is used to optimize the proposed objective function. Comprehensive comparisons are taken among the proposed method, other Evolutionary Algorithms (EAs), and conventional signal processing techniques, which show BSA with Local Probability likelihood (BSA-LP) has the best performance on the estimation.**

I. Introduction

In the past decade, the smart transmission systems are widely deployed all over the world. It is more and more common to have power systems interconnected to individual islands over long distances. Although interconnected transmission system decreases the reserve capacities and improves system stability, it has also brought new disadvantages. One of the major problems is that the conflicts between large transfer capacity and weak interconnection cause LFO among generators, which further leads to negative effects on power system stability [1][2]. Therefore, it is an important task to effectively and accurately estimate the parameters of the LFO signal. Based on these estimated parameters, fault diagnosis could be performed immediately to improve the dynamic stability in long-distance-transmission capability [3][4].

Generally, LFO is a combination of several damping sinusoidal signal, where the frequency varies in the range between 0.1 to 2.0 Hz. In some cases, the LFO also creates a rhythmic pulse or sweep in the grid. Referring to the range and magnitude of LFO, the modes of the LFO components can be divided into two categories: local modes having a range of 1.0 to 2.0 Hz and inter-area modes having a range of 0.1 to 1.0 Hz [5]. Therefore, correctly estimating the frequency LFO could provide a reference information for the system operator to locate the fault in the grid. Besides the frequency of LFO, the damping ratio is another critical parameter to be estimated. LFO signals with small damping ratio are usually caused by serious systems faults, where the effects remain in the grid for a long period. With a fast estimation on the damping ratio, the serious faults could be isolated from the grid [6][7].

Due to the importance of LFO estimation, a large number of approaches have been developed, including two types: modal analysis and measurement-based analysis [8]. Modal analysis was employed by IEEE Task force to identify the electromechanical modes of the power system stability based on LFO. Eigen-analysis, which applies a linearised time-invariant model, is one of the most effective tools in modal analysis to evaluate modal information [9]. However, the accuracy of the dynamic models and the parameters of the system components affect the validation of the analysis. The computation becomes more complex and time consuming when a full-state eigenvalue analysis is applied. Recently, Methods of Normal Forms (MNF) have been applied to eigenanalysis providing a novel method of dealing with non-linear behaviours.

This research transfers the estimation of LFO parameters to an optimization problem, which regresses the parameters based on Least Mean Square (LMS) [10]. However, the computational complexity of the proposed scheme is significantly higher than conventional measurement-based analysis methods. Therefore, a fast converge optimization algorithm, BSA, is adopted to estimate the parameters of LFO. BSA is developed from the Bacterial Foraging Algorithm (BFA) [11], which simply describes the chemotaxis behaviour of a colony of bacteria. With more comprehensive foraging models, BSA incorporates the mechanisms of quorum sensing [12]. Chemotaxis behaviour offers the basic search principle, which consists of two basic foraging patterns, tumble and run. The biased random walk performs the "local search" in the searching space, and the tumble process selects a better direction to search [13]. Meanwhile, the quorum sensing allows BSA to escape from local optima, which is a two-fold operation that can either attract a bacterium to the optimal location or repel it away from the location where bacteria are concentrated. According to our previous studies, BSA demonstrates a superior performance in comparison with other evolutionary algorithms, such as Genetic Algorithm (GA) [14], Particle Swarm Optimizer (PSO) [15], Fast Evolutionary Programming (FEP) [16] and Group Search Optimizer (GSO)

978-1-7281-6929-3/20/$31.00 ©2020 IEEE

[17].

In the experimental studies, this paper presents the simulation undertaken on three test cases, including single mode, multiple modes and LFO with DC offset. The results of BSA-LP are also compared with other EAs and Prony's method. The experimental results demonstrate that BSA-LP not only provides a reliable estimation with the minimal error and fast convergence speed, but also has a stable performance in noisy environment.

II. Low Frequency Oscilliation and Probability Likelihood

A. Estimation on LFO Parameters

A LFO signal $Y(t)$ can be described as a combination of multiple models. Each mode is represented as a damping sinusoidal signal:

$$\bar{Y}(t) = \sum_{m=1}^{N_{\mathrm{m}}} \bar{A}_m e^{-\bar{s}_m t} \sin(\bar{\omega}_m t + \bar{\phi}_m) \tag{1}$$

where N_{m} is the number of models in the signal, $\bar{A}_m$ and $\bar{s}_m$ are the amplitude and damping ratio in the m^{th} model, $\bar{\omega}_m$ and $\bar{\phi}_m$ are the angular frequency and initial phase of the oscillation in the m^{th} model.

The estimation of LFO parameters can be transferred to a curve fitting problem, which makes predictions for the target variable $Y = \{y_1, y_2, \cdots, y_N\}^\top$ given a new value of input time sequence $T = \{t_1, t_2, \cdots, t_N\}^\top$. Therefore, the estimated LFO signal is expressed as:

$$Y(t) = \sum_{m=1}^{N_m} A_m e^{-s_m t} \sin(\omega_m t + \phi_m) \tag{2}$$

where A_m, s_m, ω_m and ϕ_m are the parameters of estimated oscillation in the m^{th} model. A vector w is used to express the estimated LFO parameters as:

$$\begin{aligned} w &= [A_1, \cdots, A_{N_m}, s_1, \cdots, s_{N_m}, \\ &\quad \omega_1, \cdots, \omega_{N_m}, \phi_1, \cdots, \phi_{N_m}]. \end{aligned} \tag{3}$$

During the regression, the uncertainty over the value of the target variable is expressed as a probability distribution. The samples should be evenly distributed along the regressed expression. As a the error are mainly caused by random noise, the corresponding value of the y has a Gaussian distribution with a mean equal to the actual value $\bar{Y}(t, w)$ of the (1) as:

$$p(y|t, w, \beta) = \mathcal{N}\left(y|\bar{y}(t, w), \beta^{-1}\right) \tag{4}$$

where precision parameter β corresponds to the inverse variance of the distribution.

To determine the value of unknown parameters w and β by maximum likelihood, we assume the data are drawn independently from the Gaussian distribution, the likelihood function is given by:

$$p(y|t, w, \beta) = \prod_{n=1}^{N} \mathcal{N}\left(y_n|\bar{y}_n(t_n, w), \beta^{-1}\right). \tag{5}$$

The sample period of LFO should be selected large enough to guarantee the estimation accuracy. Therefore, the number of samples, N, is increased as well. To reduce the computation complexity, a sample filter based on probability is introduced to the likelihood function.

For the case of a single real-value variable t, the Gaussian distribution with mean value μ and deviation σ is defined by:

$$\mathcal{N}(t|\mu, \sigma^2) = \frac{1}{\sqrt{2\pi\sigma^2}} \exp\left\{-\frac{(t-\mu)^2}{\sigma^2}\right\}. \tag{6}$$

Conventional polynomial regression uses the LMS to find the best fitting, which is based on the logarithm likelihood:

$$\begin{aligned} \ln p(y|t, w, \beta) &= -\frac{\beta}{2} \sum_{n=1}^{N} \{\bar{y}(t_n, w) - t_n)\}^2 \\ &\quad + \frac{N}{2} \ln \beta - \frac{N}{2} \ln(2\pi). \end{aligned} \tag{7}$$

Therefore, the maximum likelihood to determine the precision parameter β of the Gaussian condition distribution is transferred to a maximization on:

$$\frac{1}{\beta} = \frac{1}{N} \sum_{n=1}^{N} \{\bar{y}(t_n, w) - y_n\}^2. \tag{8}$$

However, the evaluation based on LMS algorithm is not efficient when the number of points N is selected too large. Therefore, this research proposes a filter technique to select estimation regions based on MM.

B. MM Filter

The MM consists two basic operators, which are erosion and dilation [18]. For these two operators, only addition and subtraction calculation are used [19]. Thus, MM is an effective algorithm to extract features of the target signal. The erosion ($\ominus$) and dilation ($\oplus$) are expressed as:

$$\begin{aligned} &f \ominus g(n) = \\ &\quad \min_s \{f(n+s) - g(s) | (n+s) \in \mathcal{D}_f, s \in \mathcal{D}_g\} \end{aligned} \tag{9}$$

$$\begin{aligned} &f \oplus g(n) = \\ &\quad \max_s \{f(n+s) + g(s) | (n+s) \in \mathcal{D}_f, s \in \mathcal{D}_g\} \end{aligned} \tag{10}$$

where f is the target signal, g is a designed structure element, $\mathcal{D}_f$ and $\mathcal{D}_g$ are the domains of f and g, respectively. By combining erosion and dilation operators, two MM filters are further created, which are opening ($\circ$) and closing ($\bullet$):

$$f \circ g = (f \ominus g) \oplus g \tag{11}$$

$$f \bullet g = (f \oplus g) \ominus g. \tag{12}$$

The MM filter is used to select the regions with minimal gradient in the original signal to process the regression, which aims to reduce the computational complexity. In a damping sinusoidal signal, the dip and peak regions have minimal gradient. These regions contain sufficient information to support the regression. In this research, the sample rate of original signal is 50Hz, which means one sample is taken in each cycle from a power system with frequency of 50 Hz. To perform the

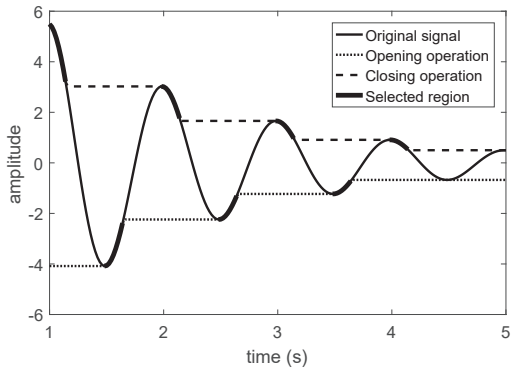

Fig. 1. Estimation region select by MM filter

MM filter, a sphere SE, g_s, is constructed with radius of 30 samples. Then opening and closing operations are applied to the original signal. The results after opening ($\bar{Y}_{\rm op}$) and closing ($\bar{Y}_{\rm cl}$) are calculated as:

$$\bar{Y}_{\rm op} = \bar{Y} \circ g_s \tag{13}$$

$$\bar{Y}_{\rm cl} = \bar{Y} \bullet g_s. \tag{14}$$

The overlapped area between $\bar{Y}_{\rm op}$ and $\bar{Y}$, and area between $\bar{Y}_{\rm cl}$ and $\bar{Y}$ are regions with minimal gradient. These regions are represented as $\bar{Y}_{\rm MM}$ in this study. The $\bar{Y}_{\rm op}$, $\bar{Y}_{\rm cl}$, $\bar{Y}$ and $\bar{Y}_{\rm MM}$ are illustrated in Fig. 1 as a demonstration.

III. Bacterial Swarm Algorithm

A. Chemotaxis

The chemotaxis behavior can be modeled by a tumble-run process that consists of a tumble step and several run steps. The tumble-run process follows a gradient searching principle, which indicates that the position of the bacterium is updated in the run steps by the gradient information provided by the tumble step. Determining the rotation angle taken by a tumble action in an *n*-dimensional search space can be described as follows. Suppose the $p^{\rm th}$ bacterium, in the tumble-run process of the $k^{\rm th}$ iteration, has a current position $X_p^k \in \mathbb{R}^n$. The objective of the optimization is to find the minimum of $F(X_p^k)$. The bacterium also has a rotation angle $\varphi_p^k = \left(\varphi_{p1}^k, \varphi_{p2}^k, ..., \varphi_{p(n-1)}^k\right) \in \mathbb{R}^{n-1}$ and a tumble length $D_p^k(\varphi_p^k) = \left(d_{p1}^k, d_{p2}^k, ..., d_{pn}^k\right) \in \mathbb{R}^n$, which can be calculated from φ_p^k via a polar-to-cartesian coordinate transform:

$$\begin{aligned} d_{p1}^k &= \prod_{i=1}^{n-1} \cos\left(\varphi_{pi}^k\right), \\ d_{pj}^k &= \sin\left(\varphi_{p(j-1)}^k\right) \prod_{i=p}^{n-1} \cos\left(\varphi_{pi}^k\right) \quad j = 2, 3, ..., n-1 \\ d_{pn}^k &= \sin\left(\varphi_{p(n-1)}^k\right). \end{aligned} \tag{15}$$

In the polar-to-cartesian coordinate transform, an arbitrary vector in the n-dimensional space can be represented by $n-1$ angles and a normalized distance to the original point.

The maximal rotation angle $\varphi_{\max}$ is related to the number of the dimensions of the objective function, which can be formulated as:

$$\varphi_{\max} = \frac{\pi}{\lfloor \sqrt{n+1} \rfloor} \tag{16}$$

where n is the number of dimensions and $\lfloor \cdot \rfloor$ denotes the operation which rounds the element to the nearest integer towards minus infinity. By introducing (16), the maximal rotation angle is restricted with the increase of dimension. As a result, the algorithm is easier to converge to the optima in high-dimensional environment, when it finds a heading angle with an effective direction.

In the tumble-run process of the $k^{\rm th}$ iteration, the $p^{\rm th}$ bacterium generates a random rotation angle, which falls in the range of $[0, \varphi_{\max}]$. A tumble action takes place in an angle expressed as:

$$\hat{\varphi}_p^k = \varphi_p^k + r_1 \varphi_{\max}/2 \tag{17}$$

where $r_1 \in \mathbb{R}^{n-1}$ is a uniform random sequence with a range of $[-1, 1]$. The run action immediately follows the tumble action. Because the run action will be performed more than once, the position X_p^k is recorded as $\hat{X}_p^{k,0}$, which indicates the position of the $p^{\rm th}$ bacterium at the beginning of the $k^{\rm th}$ iteration.

Once the angle is determined by the tumble step, the bacterium will run for a maximum of $N_{\rm c}$ run steps. If at the $N_{\rm f}^{\rm th}$ ($N_{\rm f} < N_{\rm c}$) run step, the bacterium finds a position which has a better fitness value than the current one, the run process also stops. The position of the $p^{\rm th}$ bacterium is updated at the $h^{\rm th}$ ($h \geq 1$) run step in the following way:

$$\hat{X}_p^{k,h} = \hat{X}_p^{k,h-1} + r_2 D_p^k(\hat{\varphi}_p^k) \tag{18}$$

where $r_2 \in \mathbb{R}$ is a normally distributed random number generated from $\mathcal{N}(0, D_{\max})$, $D_{\max}$ is the maximal step length of a run, and $\hat{X}_p^{k,h}$ is the position of the $p^{\rm th}$ bacterium after the $h^{\rm th}$ run step. For convenience of description, the position of the $p^{\rm th}$ bacterium beginning immediately after the tumble-run process of the $k^{\rm th}$ iteration is denoted by $\hat{X}_p^{k,N_{\rm f}}$, $N_{\rm f} \leq N_{\rm c}$.

The rotation angle is updated after each iteration. The tumble angle of the $p^{\rm th}$ bacterium at the beginning of the $(k+1)^{\rm th}$ iteration is expressed as φ_p^{k+1}, which has the same value as $\hat{\varphi}_p^k$.

B. Quorum sensing

Inspired by PSO, the positions of the bacteria moving by attraction are updated as follows:

$$X_p^{k+1} = \hat{X}_p^{k,N_{\rm f}} + r_3(X_{\rm best} - \hat{X}_p^{k,N_{\rm f}}) \tag{19}$$

where $r_3 \in \mathbb{R}$ is a normally distributed random number with a range of $[-1, 1]$, which describes the strength of bacterial attraction, and $X_{\rm best}$ indicates the position of the current best global solution updated after the evaluation of each function.

In BSA, a small number of the bacteria are randomly selected to be repelled. To measure the degree of repelling, a repelling rate is defined by ζ, *i.e.*, in each iteration, 100ζ percent of the bacteria are processed by repelling. Accordingly

TABLE I
PSEUDO CODE OF BSA

Set $k := 0$;
Randomly initialise bacterial positions;
WHILE (termination conditions are not met)
  FOR (each bacterium p)
    Tumble: Turn the heading angle randomly by (17).
      Set $h := 1$
    Run:
      WHILE ($h < N_{\mathrm{c}}$)
        Move the bacterium towards the heading angle to the new position $\hat{X}_p^{k,h}$ by equation (18). If the fitness value at current position is worse than that at previous position, set $h := N_{\mathrm{c}}$; otherwise, increase h by 1;
      END WHILE
  END FOR
  Quorum Sensing:
    (1-ζ)100% of the bacteria are attracted to the global optimum by equation (19), ζ 100% of bacteria are repelled by equation (20);
  $k := k + 1$;
END WHILE

the attraction rate is $100(1-\zeta)$ percent. The repelling process is based on the random searching principle. If the p^{th} bacterium shifts into the repelling process, a random angle in the range of $[0, \pi]$ is generated. The bacterium is thereby "moved" to a random position following this angle in the search space, which can be described as:

$$X_p^{k+1} = \hat{X}_p^{k,N_{\mathrm{f}}} + r_4 D_p^k (\hat{\varphi}_p^k + \pi/2) \tag{20}$$

where $r_4 \in \mathbb{R}^n$ is a normally distributed random sequence which drawn from $\mathcal{N}(0, D_{\mathrm{range}})$, and D_{range} is the range of the search space. The pseudo code for BSA is listed in Table I.

IV. SIMULATION STUDIES

A. Algorithm settings

The experimental studies compare the proposed algorithm with conventional analysis methods, such as Discrete Fourier Transform (DFT) and Prony's Method (PM). As an effective frequency domain analysis tool, DFT were widely used to measure the frequency of LFO, even the LFO is not a periodic signal. For DFT, the window size covers full range of the signal. Prony's method extracts valuable information from a uniformly sampled signal and builds a series of damping complex exponential sinusoid signals. The number of modes (n) must be specified before applying PM analysis (PM-n). When n is set to a value lager than actual number of modes, the reconstructed LFO signal will have a form matching with original signal. However, the estimated parameters will not present the actual components in the signal.

Meanwhile, we also compare the BSA-LP with other EAs, such as Genetic Algorithm (GA) and Particle Swarm Optimizer (PSO). The population sizes of these three algorithms are all set to 50, and the number of iterations are set to 1,000. Therefore, the objective functions are evaluated 50,000 times for each estimation. The mutation probability of GA is set to 0.1. The inertia weight (ω), local attraction factor (c_1) and global attraction factor (c_2) are set to 0.73, 2.05 and 2.05, respectively [20].

TABLE II
SETTING OF LFO PARAMETERS

Parameter	Minimal value	Maximal value
Amplitude ($\bar{A}$)	0	10
Damping ratio ($\bar{s}$)	0	1
Frequency ($\bar{f} = 2\pi/\bar{\omega}$)	0.1Hz	2.0Hz
Initial phase ($\bar{\phi}$)	$-\pi/2$	$\pi/2$

TABLE III
EXPERIMENTAL RESULTS OF CASE I: SINGLE MODE ESTIMATION

Algorithm	e_A	e_s	e_f	e_ϕ	e_{L}	e_{LP}
DFT	84.27	NA	3.31	NA	NA	NA
PM-1	11.72	27.65	1.89	7.42	9.53E0	NA
GA	0.20	**0.36**	0.04	0.66	**1.25E-1**	1.23E-1
PSO	0.40	0.56	0.19	0.58	1.51E-1	2.49E-1
BSA	**0.20**	0.45	**0.03**	**0.50**	**1.25E-1**	**1.22E-1**

B. Case I: Single mode estimation

In this experiment, 1,000 LFO signals are generated individually. The amplitude, damping ratio, frequency and initial phase of each signal are randomly selected from the ranges listed in Table II. Meanwhile, 30 dB white noise is also added to each signal. All algorithms adopted for comparison and BSA-LP are applied to estimate the parameters of these LFO signals.

The numerical results are listed in Table III. The comparison for parameter estimation is based on Mean Absolute Percentage Error (MAPE):

$$e = \frac{1}{N_{\mathrm{E}}} \sum_{i=1}^{N_{\mathrm{E}}} \frac{|\bar{Z}_i - Z_i|}{|\bar{Z}_i|} \times 100\% \tag{21}$$

where N_{E} is the number of experiments, $\bar{Z}_i$ and Z_i are the actual parameter and estimated parameter in the i^{th} experiment. Meanwhile, the average LMS error (e_{L}) and average LMS error of the selected region (e_{LP}) are also compared in this table.

It can be found that the amplitude (0.20%), frequency (0.03%) and phase angle (0.5%) estimated by BSA-LP has the minimal MAPE. The GA estimates a better damping ratio (0.36%) than BSA-LP (0.45%) in this experiment. The LFO signal reconstructed by BSA-LP also has the minimal e_{L} error (1.25E-1) and e_{LP} error (1.22E-1), which is nearly same as the error of the signal reconstructed by GA (1.25E-1). As the objective function in this research is a multimodal funtion, which contains many local optima around global optimum. Therefore, PSO is not suitable to solve this optimization problem, due to the lack on mutation scheme to keep the population diversity. The signal reconstructed by PSO has lager errors (1.51E-1). For conventional analysis methods, DFT only estimates the frequency with acceptable error (3.31%). By applying the PM-1, the LFO signal can be reconstructed with a small error (9.53E0). The numerical

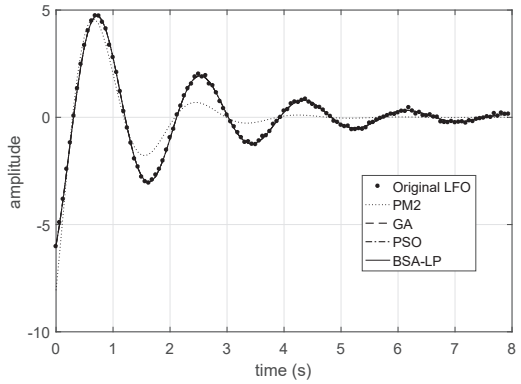

Fig. 2. Original and Reconstructed LFO signal with single mode

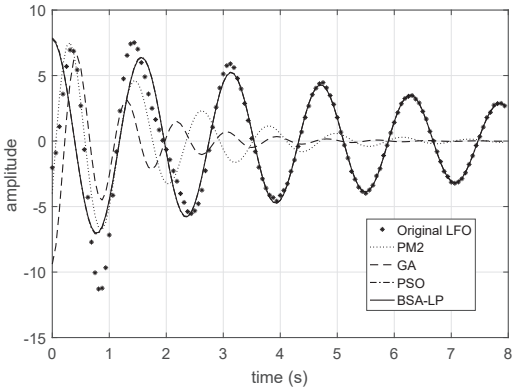

Fig. 3. Original and Reconstructed LFO signal with 2 modes

TABLE IV
EXPERIMENTAL RESULTS OF CASE II: MULTIPLE MODE ESTIMATION

Algorithm	2 modes		3 modes	
	e_L	e_{LP}	e_{L}	e_{LP}
PM-2 & PM-3	4.98E2	N/A	5.00E2	NA
GA	1.64E1	1.62E1	2.49E1	2.46E1
PSO	7.27E1	7.23E1	1.36E2	1.30E2
BSA-LP	**3.14E0**	**3.08E0**	**1.17E1**	**1.15E1**

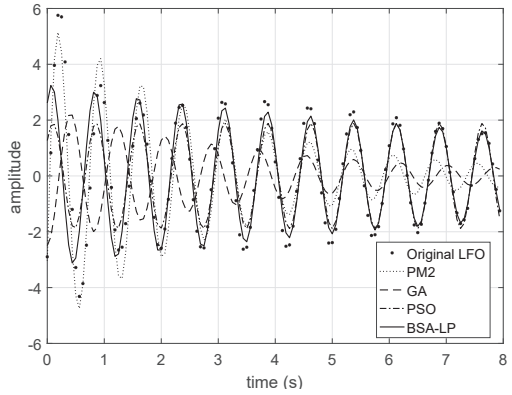

Fig. 4. Original and Reconstructed LFO signal with 3 modes

results indicate PM is not suitable to estimate the damping ratio (27.65%) and amplitude (11.72%). The original LFO signals and those reconstructed by PM1, GA, PSO and BSA-LP with single mode are illustrated in Fig. 2. In this figure, the signals reconstructed by GA, PSO and BSA-LP are overlapped due to the small e_{L} error.

C. Case II: Multiple mode estimation

The LFO signal adopted in the second experiment consists of multiple modes. The algorithms are applied to estimate the parameter of each sub mode. In order to fully evaluate the proposed algorithm, the numbers of modes are selected as 2 and 3 in this experiment.

Table IV lists the error comparison among estimation algorithms. From the result, it can be found that the signal reconstructed by BSA-LP has minimal errors both on 2 modes (3.14E0) and 3 modes (1.17E1) LFO signals. GA (1.64E1 and 2.49E1) outperforms PSO (7.27E1 and 1.36E2), due to the population diversity. PM has the worst performances (4.99E2 and 5.00E2) in two experiments. Meanwhile, we also compare the standard deviation of BSA-LP 1,000 separate runs. The results are 1.21E1 and 3.09E, which shows the performance of BSA-LP is stable. The original LFO signals and those reconstructed by PM1, GA, PSO and BSA-LP with 2 modes and 3 modes are illustrated in Fig. 3 and Fig. 4. From these two figures, it also can be found that all estimation algorithms are affected by the noise and mode in the signal. As the window for the estimation is around 10 seconds, the estimation algorithms focuses on the later stage of the signal, which is stable and easy to achieve a better accuracy. Therefore, BSA-LP not estimate the peak values of the amplitude of the LFO signal in the early stage. In contrast, PM2 more focus on later stage or the signal.

D. Case III: LFO with DC offset

In real applications, LFO signals are usually accompanied with DC offset, which causes the estimation procedure extremely difficult. In traditional research, DC offset cancellation filter or algorithm are usually used as pre-processing progress. However, the proposed scheme is able to be applied to estimate the parameters of LFO and DC offset simultaneously. The LFO model with DC offset $Z(t)$ can be presented as:

$$Z(t) = Y(t) + A_{\mathrm{D}} e^{-s_{\mathrm{D}} t} \tag{22}$$

where $Y(t)$ is the LFO signal described in Section II, A_{D} and s_{D} are the amplitude and ratio of the DC offset. In this experiment, A_{D} is randomly selected in the range of $[0, 10]$, and s_{D} is randomly selected in the range of $[0, 1]$.

The experiment result on case III is listed in Table V. The detailed LFO parameters are not listed in this table. In this case, PM is not suitable to estimate the parameters as it only decomposes the LFO to damping sinusoidal signal.

TABLE V
EXPERIMENTAL RESULTS OF CASE III: ESTIMATION ON LFO AND DC OFFSET

Algorithm	A_{D}	s_{D}	e_{L}	e_{LP}
GA	1.66	1.50	1.22E1	1.15E1
PSO	6.34	9.10	1.30E2	1.15E2
BSA-LP	**1.65**	**1.47**	**3.41E0**	**3.22E0**

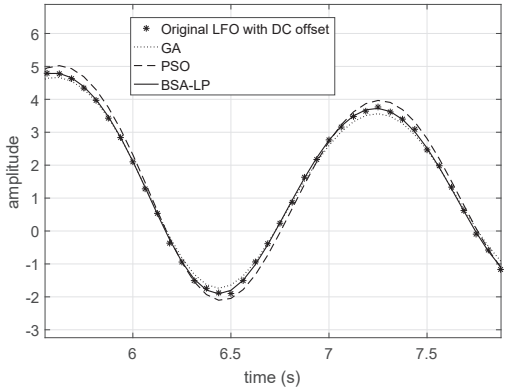

Fig. 5. Original and Reconstructed damping LFO signal with 2 modes

From the numerical comparison, it can be found that BSA-LP has the minimal e_{L} (3.41E0) and e_{LP} (3.22E0) errors. The estimated errors of A_D and s_D are 1.65% and 1.47%, respectively. Due to the accurate estimated parameters, the DC offset can be removed effectively. GA has nearly the same performance (1.22E1) as BSA-LP, which shows a great potential on multi-modal parameter estimation. The errors of parameter estimation on A_D and s_D are 1.66% and 1.50%. Among these three algorithms, PSO has the worst performance (1.30E2), and fails to estimate the parameters of DC offset (6.34% and 9.10%). The original LFO signal with DC offset and those reconstructed by GA, PSO and BSA-LP are illustrated in Fig. 5.

V. CONCLUSION

In order to support fault diagnosis in power systems, this research proposes a novel regression scheme to estimate the parameters to LFO. By applying the MM filter, fitting segments are selected from original LFO signal, which greatly reduces the computational complexity. Then BSA is applied to optimize the probability likelihood between the reconstructed and original signal. The experiment results indicate the proposed scheme has a better performance than conventional PM, especially in the noisy environment. On three-mode estimation, the estimation error of BSA-LP is 98% less than PM. Compared with other EAs, such as GA and PSO, BSA also has a better accuracy. Meanwhile, the LFO signal with DC offset is also analysed is this research. The proposed scheme is able to estimate the parameters of DC offset and LFO simultaneously with a superior performance.

VI. ACKNOWLEDGEMENT

The work is jointly funded by Research Project of Qingyuan Power Supply Bureau, China Southern Grid (GDKJXM20183525) and the Fundamental Research Funds for Central Universities, South China University of Technology (2019MS014).

REFERENCES

[1] Y. Yu, S. Grijalva, J. J. Thomas, L. Xiong, P. Ju, and Y. Min. Oscillation energy analysis of inter-area low-frequency oscillations in power systems. *IEEE Transactions on Power Systems*, 31(2):1195–1203, March 2016.

[2] A. Q. Zhang, L. L. Zhang, M. S. Li, and Q. H. Wu. Identification of dominant low frequency oscillation modes based on blind source separation. *IEEE Transactions on Power Systems*, PP(99):1–1, 2017.

[3] Z. Ke, J. Zhang, and R. Raich. Low-frequency current oscillation reduction for six-step operation of three-phase inverters. *IEEE Transactions on Power Electronics*, 32(4):2948–2956, April 2017.

[4] H. Villegas Pico, J. D. McCalley, A. Angel, R. Leon, and N. J. Castrillon. Analysis of very low frequency oscillations in hydro-dominant power systems using multi-unit modeling. *IEEE Transactions on Power Systems*, 27(4):1906–1915, Nov 2012.

[5] M. Hatami, M. Farrokhifard, and M. Parniani. A non-stationary analysis of low-frequency electromechanical oscillations based on a refined margenau-hill distribution. *IEEE Transactions on Power Systems*, 31(2):1567–1578, March 2016.

[6] C. Abbate, G. Busatto, A. Sanseverino, F. Velardi, and C. Ronsisvalle. Analysis of low- and high-frequency oscillations in igbts during turn-on short circuit. *IEEE Transactions on Electron Devices*, 62(9):2952–2958, Sept 2015.

[7] H. Ye, Y. Liu, P. Zhang, and Z. Du. Analysis and detection of forced oscillation in power system. *IEEE Transactions on Power Systems*, 32(2):1149–1160, March 2017.

[8] J. Z. Yang, C. W. Liu, and W. G. Wu. A hybrid method for the estimation of power system low-frequency oscillation parameters. *IEEE Transactions on Power Systems*, 22(4):2115–2123, Nov 2007.

[9] D. Lauria and C. Pisani. On hilbert transform methods for low frequency oscillations detection. *IET Generation, Transmission Distribution*, 8(6):1061–1074, June 2014.

[10] M. Beza and M. Bongiorno. A modified rls algorithm for online estimation of low-frequency oscillations in power systems. *IEEE Transactions on Power Systems*, 31(3):1703–1714, May 2016.

[11] MS Li, TY Ji, WJ Tang, QH Wu, and JR Saunders. Bacterial foraging algorithm with varying population. *Bio Systems*, 100(3):185197, June 2010.

[12] S. Cheng, L. L. Zhao, and X. Y. Jiang. An effective application of bacteria quorum sensing and circular elimination in mopso. *IEEE/ACM Transactions on Computational Biology and Bioinformatics*, 14(1):56–63, Jan 2017.

[13] M. S. Li, T. Y. Ji, and Q. H. Wu. Discrete paired-bacteria optimizer for solving traveling salesman problem. In *2013 IEEE Symposium on Computational Intelligence in Production and Logistics Systems (CIPLS)*, pages 86–91, April 2013.

[14] T. Mareda, L. Gaudard, and F. Romerio. A parametric genetic algorithm approach to assess complementary options of large scale windsolar coupling. *IEEE/CAA Journal of Automatica Sinica*, 4(2):260–272, 2017.

[15] J. Li, J. Zhang, C. Jiang, and M. Zhou. Composite particle swarm optimizer with historical memory for function optimization. *IEEE Transactions on Cybernetics*, 45(10):2350–2363, Oct 2015.

[16] N. Sinha, R. Chakrabarti, and P. K. Chattopadhyay. Fast evolutionary programming techniques for short-term hydrothermal scheduling. *IEEE Transactions on Power Systems*, 18(1):214–220, Feb 2003.

[17] S. He, Q. H. Wu, and J. R. Saunders. Group search optimizer: An optimization algorithm inspired by animal searching behavior. *IEEE Transactions on Evolutionary Computation*, 13(5):973–990, Oct 2009.

[18] Anjanappa C. and Sheshadri. H. S. Development of mathematical morphology filter for medical image impulse noise removal. In *2015 International Conference on Emerging Research in Electronics, Computer Science and Technology (ICERECT)*, pages 311–318, Dec 2015.

[19] Z. Ji, Q. Zeng, J. Liao, and Q. H. Wu. A novel mathematical morphology filter for the accurate fault location in power transmission lines. In *TENCON 2009 - 2009 IEEE Region 10 Conference*, pages 1–6, Jan 2009.

[20] M. Clerc and J. Kennedy. The particle swarm - explosion, stability, and convergence in a multidimensional complex space. *IEEE Transactions on Evolutionary Computation*, 6(1):58–73, Feb 2002.